# Quantum confined acceptors and donors in InSe nanosheets

G. W. Mudd, A. Patanè, Z. R. Kudrynskyi, M. W. Fay, O. Makarovsky, L. Eaves, Z. D. Kovalyuk, V. Zólyomi, and V. Falko

---

### Articles you may be interested in

Nonlinear and saturable absorption characteristics of amorphous InSe thin films
J. Appl. Phys. **107**, 033115 (2010); 10.1063/1.3298500

Barrier width dependence of the donor binding energy of hydrogenic impurity in wurtzite InGaN/GaN quantum dot
J. Appl. Phys. **106**, 094301 (2009); 10.1063/1.3245335

Electrical and optical properties of n- and p-InSe doped with Sn and As
J. Appl. Phys. **93**, 2301 (2003); 10.1063/1.1539558

Heat capacity of the n-InSe single crystal layered semiconductor
J. Appl. Phys. **92**, 5110 (2002); 10.1063/1.1512322

Photoluminescence of undoped and neutron-transmutation-doped InSe
J. Appl. Phys. **88**, 4654 (2000); 10.1063/1.1308066

---

# Quantum confined acceptors and donors in InSe nanosheets

G. W. Mudd,[1] A. Patanè,[1,a)] Z. R. Kudrynskyi,[2] M. W. Fay,[3] O. Makarovsky,[1] L. Eaves,[1] Z. D. Kovalyuk,[2] V. Zólyomi,[4] and V. Falko[4]

[1]School of Physics and Astronomy, The University of Nottingham, Nottingham NG7 2RD, United Kingdom
[2]Institute for Problems of Materials Science, The National Academy of Sciences of Ukraine, Chernivtsi 58001, Ukraine
[3]Nottingham Nanotechnology and Nanoscience Centre, The University of Nottingham, Nottingham NG7 2RD, United Kingdom
[4]Physics Department, Lancaster University, Lancaster LA1 4YB, United Kingdom

We report on the radiative recombination of photo-excited carriers bound at native donors and acceptors in exfoliated nanoflakes of nominally undoped rhombohedral $\gamma$-polytype InSe. The binding energies of these states are found to increase with the decrease in flake thickness, $L$. We model their dependence on $L$ using a two-dimensional hydrogenic model for impurities and show that they are strongly sensitive to the position of the impurities within the nanolayer. © 2014 Author(s). All article content, except where otherwise noted, is licensed under a Creative Commons Attribution 3.0 Unported License. [http://dx.doi.org/10.1063/1.4903738]

Van der Waals (vdW) heterostructures made by stacking atomically thin exfoliated two-dimensional (2D) crystals represent a promising class of materials[1–3] for functional electronic devices such as tunnel transistors,[4,5] resonant tunnel diodes,[6] photovoltaic sensors,[7] and light-emitting diodes (LEDs).[8] The electronic properties of these devices can be controlled by selection of the materials within the stack, the built-in strain, and/or relative orientation of the component crystalline layers.[9–13] Among the vdW crystals, InSe represents an exfoliable and stable compound that enriches the current "library" of 2D crystals (graphene, hBN, $MoS_2$, $WS_2$, etc.). It is a semiconductor with direct band gap energy that can be increased due to quantum confinement by reducing the number of layers in the crystalline sheet.[14] The observation of tuneable absorption in the near-infrared and visible spectral range,[15] and the recent reports of high-performance and bendable photodetectors,[16] $p$-$n$ junctions,[17] and FETs[18] with high room-temperature mobility ($0.1~m^2V^{-1}s^{-1}$) have demonstrated the potential of InSe for device applications. Further interest in InSe arises from its electronic band structure: as a single- or few-layer nanoflake, this compound becomes an indirect band gap semiconductor and develops a sombrero-shaped energy dispersion curve for holes near the valence-band edge.[19,20] This feature may lead to a Lifshitz transition in $p$-type InSe, i.e., a change in the Fermi-surface topology, which modifies electronic properties.[19]

Crucial to future technology developments is the understanding of the effects of dopant atoms on electronic and optical properties. Carrier localization on strongly confined dopant states could degrade the carrier mobility of FETs[18] and trapping/de-trapping of carriers at these states could increase noise levels and limit the exploitation of InSe in optical devices, such as LEDs and photodetectors,[16,17] by producing slow optical temporal responses and broad emission lines. Here, we investigate the radiative recombination of photo-excited carriers bound at donor and acceptor sites in exfoliated nanolayers of nominally undoped $\gamma$-InSe. We study their photoluminescence (PL) spectra over a range of temperatures from $T = 8~K$ to $300~K$ and show that at low temperatures, the recombining carriers are bound to native donors and acceptors whose binding energy increases significantly when the nanoflake thickness, $L$, is decreased to a few nanometers. Further strong changes in the binding energies can be expected as $L$ is reduced below the critical value ($\sim 10~nm$) for the direct-to-indirect band gap crossover due to the emergence of a strongly modified band structure.[19,20]

Our InSe crystals were grown using the Bridgman method from a polycrystalline melt of $In_{1.03}Se_{0.97}$. The $\gamma$-polytype crystal structure of InSe was probed by X-ray diffraction (XRD) using a DRON-3 X-ray diffractometer in a monochromatic Cu-K$\alpha$ radiation of wavelength $\lambda = 1.5418~\text{Å}$. As shown in Figure 1(a), the primitive unit cell contains three InSe layers, each consisting of four covalently bonded monoatomic sheets in the sequence Se-In-In-Se of thickness $L = 8.320~\text{Å}$; along the $c$-axis, the primitive unit cell has a lattice constant of $c = 24.961~\text{Å}$ and within each $a$-$b$ plane, atoms form hexagons with lattice parameter $a = 4.002~\text{Å}$. The InSe nanosheets were prepared from the as-grown crystals by mechanical exfoliation using adhesive tape. They were then deposited on a silicon oxide/Si substrate and immersed in acetone to remove the tape residuals. The thickness of the nanosheets was measured by atomic force microscopy (AFM) in tapping mode under ambient conditions. Energy-dispersive X-ray (EDX) studies were performed on the bulk InSe layers using an Oxford Instruments INCA EDX system. The experimental set-up for the $\mu$PL studies comprised a He-Ne laser ($\lambda = 633~nm$), an XY linear positioning stage, an optical confocal microscope, and a spectrometer with 150 groves/mm gratings, equipped with a charge-coupled device (CCD). The laser beam was focused to a diameter $d \sim 1~\mu m$ using a 100× objective, and the $\mu$PL spectra were measured at low power ($P < 10~mW$) to minimize lattice heating. The $\mu$PL maps were produced by using a scanning mirror above the objective and with the flake mounted inside a cold-finger optical cryostat.

a)Author to whom correspondence should be addressed. Electronic mail: amalia.patane@nottingham.ac.uk
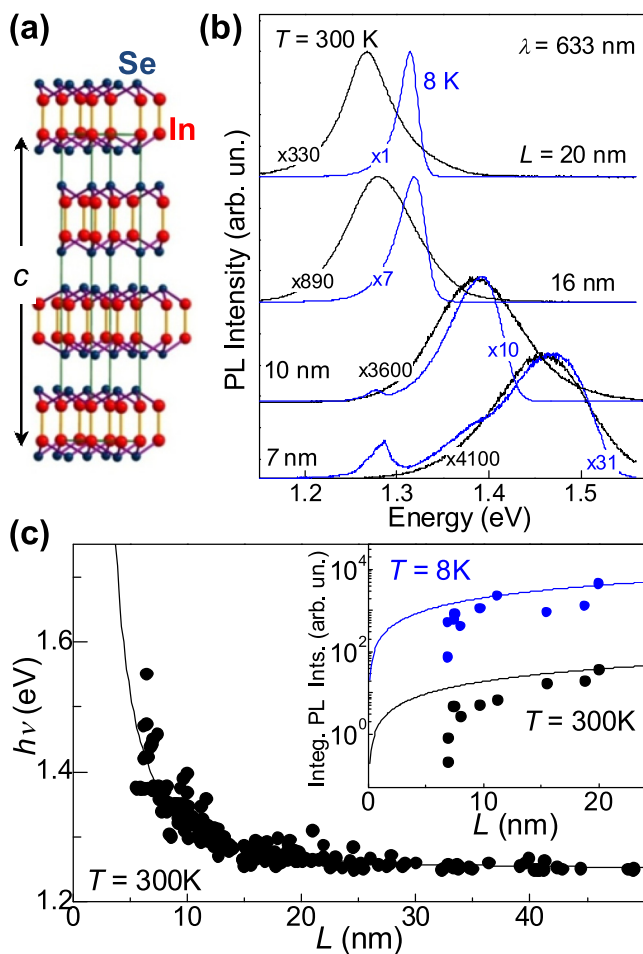
**(a)**



**(b)**



**(c)**



FIG. 1. (a) Crystal structure of $\gamma$-InSe. (b) Normalized $\mu$PL spectra of $\gamma$-InSe nanosheets with thickness $L$ in the range of 7–20 nm at $T = 8$ K (blue) and $T = 300$ K (black) ($P = 0.1$ mW and $\lambda = 633$ nm). The PL band at $h\nu = 1.29$ eV in the nanosheet with $L = 7$ nm is due to the spurious PL contribution of thicker flakes in proximity to the nanoflake. (c) Measured $L$-dependence of the PL peak energy ($T = 300$ K). The continuous line shows the calculated dependence using an effective mass model. Inset: Dependence of the PL integrated intensity on $L$ at $T = 300$ K (black dots) and 8 K (blue dots). The lines describe the decrease in the PL intensity expected from a reduction in the amount of luminescent material with decreasing $L$.

Figure 1(b) shows the normalized $\mu$PL emission spectra of mechanically exfoliated $\gamma$-InSe nanosheets of thickness $L$ from 7 nm to 20 nm at $T = 8$ K (blue lines) and $T = 300$ K (black lines). With the decrease in $L$, both series of spectra shift to high energy and broaden; in particular, for the thinnest flakes, the energy position of the main PL band is only weakly affected by temperature. The thin nanosheets also show an additional narrow PL band at an energy $h\nu \sim 1.29$ eV, close to the PL emission energy of bulk InSe. We attribute this band to the contribution of PL from thicker InSe flakes in close proximity ($< 5\,\mu$m) to the thin nanosheets.

Figure 1(c) plots the $L$-dependence of the energy of the PL peak position at $T = 300$ K for more than 100 nanosheets. The overall blue-shift with the decrease in $L$ can be explained assuming that the carriers are confined by a square quantum well (QW) potential of infinite height,[14] i.e., $h\nu = h\nu_{3D} + \pi^2\hbar^2/2L^2\mu_{//c}$, where $h\nu_{3D} = 1.25$ eV is the measured PL peak energy of bulk InSe at $T = 300$ K, $\mu_{//c}^{-1} = 1/m_{//c}^e + 1/m_{//c}^h$ is the reduced carrier mass, $m_{//c}^e = 0.08\,m_e$

($m_{//c}^h = 0.17\,m_e$) is the electron (hole) effective mass for motion along the $c$-axis in bulk InSe,[21,22] and $m_e$ is the free electron mass (see line in Fig. 1(c)). The scatter in the data points is an indication that carrier confinement could be influenced by the roughness of the sheet and its interface with the substrate and/or crystal defects.

As shown in Figure 1(c), the strong decrease of the PL integrated intensity with decreasing $L$ is observed at both $T = 300$ K and 8 K and is significantly larger than that expected from a reduction in the thickness of the optically absorbing and luminescent material. This behaviour is similar to that reported in our previous RT PL studies.[14] It is likely that surface defects affect the temperature dependence of the PL intensity, but we do not observe a stronger thermal PL quenching in the thinner nanosheets. This can be seen in the inset of Figure 1(c) and also in Figure 2, where we compare the $T$-dependence of the $\mu$PL maps for two layers, A and B, with $L = 15$ nm (Fig. 2(a)) and 10 nm (Fig. 2(b)), respectively. The two layers have uniform thickness, as can be seen in the AFM image (Fig. 2(c)), and a uniform PL peak energy, as shown in the $\mu$PL energy map of Fig. 2(d). Layer A is brighter than layer B, but for both layers, the PL intensity decreases by a factor of $\sim 10^3$ as $T$ increases from low to room temperature (Figs. 2(e)–2(f)). Thus, we attribute the systematic decrease of the PL signal as $L$ is reduced to a direct-indirect band gap crossover rather than to

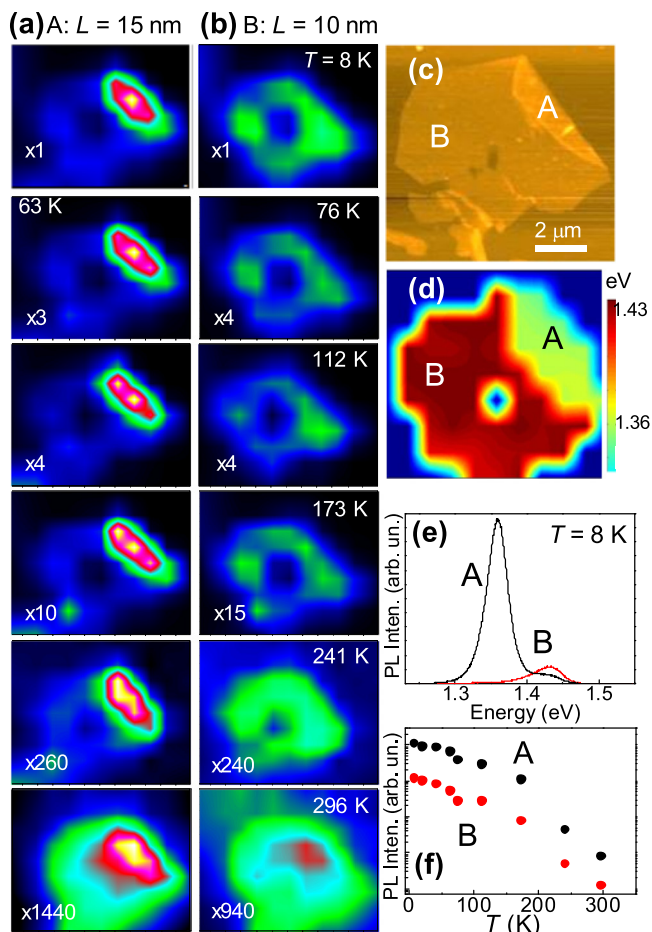**(a)** A: $L = 15$ nm  **(b)** B: $L = 10$ nm



FIG. 2. Confocal $\mu$PL maps for InSe flakes, A and B, of thickness $L = 15$ nm (a) and 10 nm (b) at various $T$ ($P = 8$ mW, $\lambda = 633$ nm). (c) AFM and (d) $\mu$PL peak energy map images. (e) PL spectra at $T = 8$ K for flakes A and B. (f) $T$-dependence of the PL peak intensity for flakes A and B.

stronger recombination at non-radiative centres. This hypothesis is supported by *ab-initio*-calculations indicating that a single layer[19] or few layers[20] of InSe have an indirect-band gap with a sombrero hat-shaped energy dispersion of holes and the valence band maximum (VBM) offset from the $\Gamma$–point, by ~10% of the $\Gamma$-$K$ and $\Gamma$-$M$ wavevectors between the $\Gamma$- and $K$-points in the Brillouin zone.

The increase in quantum confinement of carriers along the $c$-axis changes not only the band structure but can also increase the binding energy of dopant impurities due to the compression of the carrier wavefunction along the $c$-axis. Native shallow donors in bulk-InSe have binding energies of ~20 meV,[23–25] while acceptors have larger ionization energies (40 to 65 meV).[26,27] Here, we model their dependence on $L$ using a 2D hydrogenic model[28] for impurities located in the centre ($C$) and on the edge ($E$) of the well, and set the 3D donor and acceptor binding energies at $E_D = 22$ meV and $E_D = 47$ meV, respectively. Figure 3(a) plots the calculated dependence on $L$ of the 2D hydrogenic binding energy for a donor ($D_C$) and acceptor ($A_C$), and of the sum of the binding energies ($E_D + E_A$) for donor-acceptor pairs ($D_C$-$A_C$ and $D_E$-$A_C$). For a donor (acceptor) located in the central plane of the

well, the binding energy increases monotonically with the decrease in $L$. In particular, it increases towards 4 times the bulk value as $L$ is decreased to the limit of a single InSe layer, see Figure 3(b): For $L = 0$, the binding energy for the donor and acceptor is $4E_D = 88$ meV and $4E_A = 188$ meV, respectively; for a single InSe layer ($L = 0.83$ nm), these values reduce to 74 meV and 138 meV, respectively. For impurities located off-centre ($D_E/A_E$), the binding energy reaches a minimum of $E_{A,D}/4$ at the edge of the well (i.e., $E_D/4 = 5.5$ meV and $E_A/4 = 11.8$ meV) and exceeds $E_{A,D}$ for nanosheets below a critical layer thickness.

With the decrease in $L$, the calculated binding energies tend to increase and spread in energy, which can explain the corresponding spectral broadening and temperature dependence of the PL emission, shown in Figure 4(a) for representative InSe nanosheets with $L = 7$, 10, and 20 nm. It can be seen that the PL peak energy does not have a simple monotonic dependence on $T$ and the overall shift of the peak energy is dependent on $L$. To understand this behaviour, in Figure 4(b), we compare the measured PL peak energy, $h\nu$, versus $T$ with the calculated dependences for exciton ($X$), free electron to neutral-acceptor ($e$-$A$), free hole to neutral-donor ($h$-$D$), and donor-acceptor ($D$-$A$) transitions for a layer with $L = 20$ nm. In our analysis, we use the Varshni's model for the band gap energy, i.e., $E_{gL}(T) = E_{gL}(0) - \alpha T^2/(T + \beta)$, where $\alpha = 0.76$ meV K$^{-1}$ and $\beta = 480$ K are the thermal coefficients
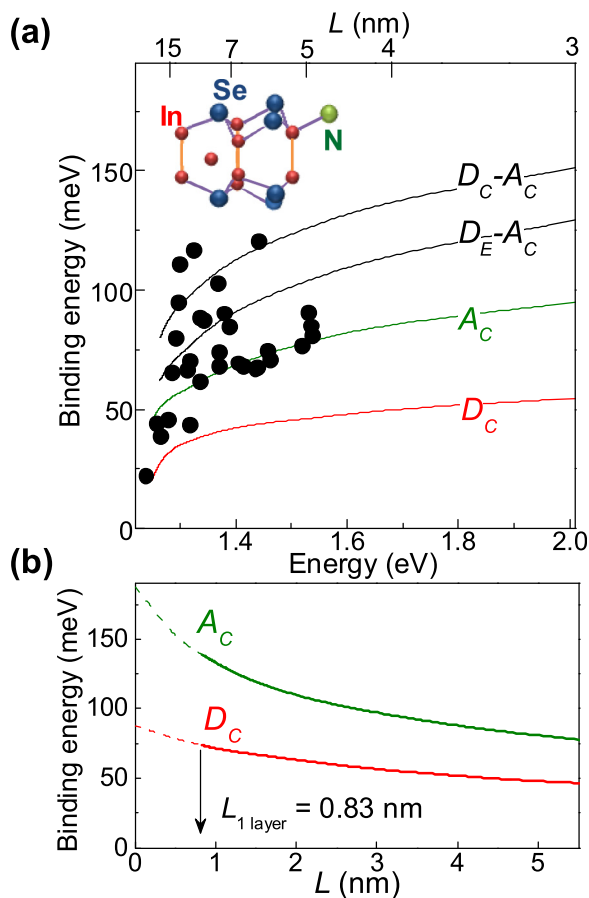


FIG. 3. (a) Calculated dependence of the binding energy of a donor ($D_C$), acceptor ($A_C$), and donor-acceptor pairs ($D_C$-$A_C$ and $D_E$-$A_C$) on the thickness $L$ (top axis) and on the band gap energy at $T = 300$ K (bottom axis) of the InSe flake. The subscripts $C/E$ refer to donors/acceptors at the centre or boundary edge of the well. The data points are estimates of the thickness dependence of the binding energies, deduced from an analysis of the PL data. Inset: In-interstitial (donor) and N-substitutional (acceptor) dopants in InSe. (b) Calculated binding energy of a donor ($D_C$) and acceptor ($A_C$) on $L$ in the limit of small $L$ (<6 nm). The vertical arrow shows the value of $L$ for a single layer of InSe ($L = 0.83$ nm).



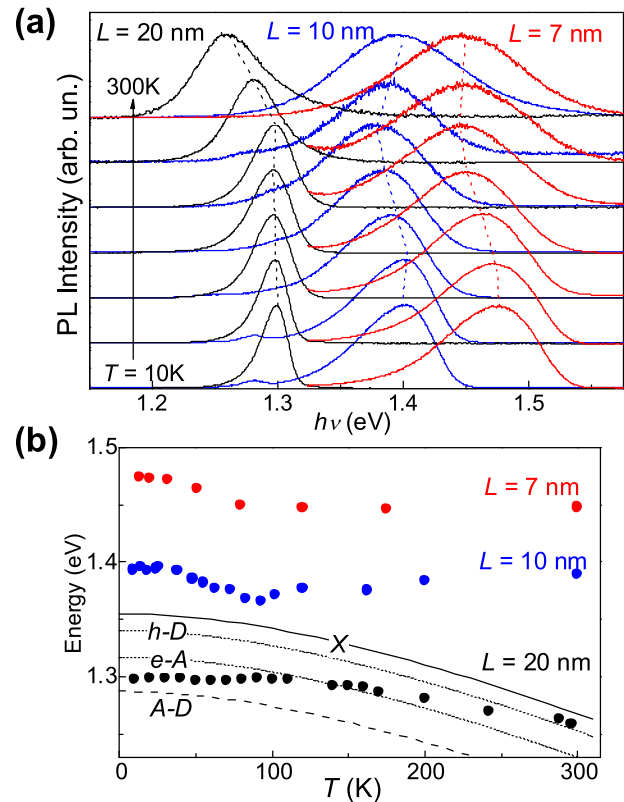FIG. 4. (a) Normalized $\mu$PL spectra for InSe nanosheets with $L = 7$ nm (red), 10 nm (blue), and 20 nm (black) in the range of $T = 10$ K–300 K ($P = 1$ mW, $\lambda = 633$ nm). Vertical dotted lines are guides to the eye and follow the $T$-dependence of the PL peak energy. (b) Dependence of the PL peak energy on $T$ (symbols) for $L = 7$, 10, and 20 nm. Lines represent the calculated $T$-dependence for the free exciton ($X$), acceptor-band ($e$-$A$), donor-band ($h$-$D$), and donor-acceptor ($D$-$A$) transitions for $L = 20$ nm. The calculated curves are for dopant atoms positioned in the centre of the well.

for bulk $\gamma$-InSe[29] and $E_{gL}(0)$ is the direct band gap energy at $T = 0$ K calculated using an infinite height-square QW potential model. We set the low temperature exciton recombination energy in bulk $\gamma$-InSe at $E_X = 1.338$ eV; finally, for the *e-A*, *h-D*, and *A-D* transitions, we use the calculated 2D donor and acceptor binding energies. From Figure 4(b), it can be seen that the PL peak energy evolves gradually from *A-D* recombinations through *e-A* and *h-D* transitions, and finally to an exciton (*X*) transition as *T* is increased from 9 K to 300 K. This gradual unbinding of the carriers leads to a blue-shift of the recombination energy, which partially compensates the red-shift predicted by Varshni's relation, thus explaining the small and non-monotonic red-shift of the measured spectra with increasing temperature.

The dopants responsible for the donor and acceptor-related recombination in our nominally undoped InSe nanosheets are likely to originate from the excess of In-atoms ($<3\%$) in the crystal growth and of N-impurities ($<1\%$), both revealed in the EDX studies of our as-grown InSe crystals. N-substitutional atoms on Se-sites are known to behave as acceptors;[28] also, In-interstitial atoms behave as shallow donors.[23–25] Because of the spectral broadening of the PL emission at small *L*, it is not possible to extract individual binding energies for donors, acceptors and/or donor-acceptor pairs from the PL spectra. Instead, we estimate an effective binding energy, $\Delta E$, from the energy difference between the low *T* values of the PL peak energy, $h\nu$, and the band gap energy, $E_{gL}$, as derived from the Varshni's dependence and the assumption that $E_{gL} = h\nu$ at $T = 300$ K.

As shown in Figure 3(a), the calculated dependence on *L* of the binding energies for acceptors, donors, and acceptor-donor pairs reproduces the general increase of $\Delta E$ with decreasing *L*. The scatter in the data is consistent with the idea that PL arises from recombination of carriers at acceptors and donors located in different positions within the flake. Further scatter in the PL emission energy may originate from modulations of the Coulomb landscape due, for example, to charged impurity pairs or impurity clustering. We note that the binding energies shown in Figure 3 are significantly larger than in the bulk, and we anticipate a further strong increase of the acceptor binding energy as the thickness of the InSe sheet is reduced to a few layers due to an interesting feature of the electronic band structure of this compound, namely, the emergence of a strongly modified flat energy dispersion curve for hole near the valence-band edge.[19,20] Also, we note that the sombrero-shaped dispersion of holes near the valence-band edge can result in a Lifshitz transition.[19] The experimental observation of this phenomenon in *p*-type InSe nanolayers may require the use of large applied electric fields to ionize the holes bound on strongly confined acceptors or else a sufficiently high acceptor density to achieve an insulator-to-metal transition.

In conclusion, we have shown that the low temperature PL emission of InSe nanoflakes is dominated by the recombination of photo-excited carriers bound at native donors and acceptors with binding energies that are sensitive to the position of the impurities within the nanolayer and that increase significantly with the decrease in flake thickness. Our results are relevant to future studies of dopant impurities in InSe and other vdW 2D crystals where acceptors or donors can be present as

unintentional or intentional dopants; of particular interest is the possibility of observing a Lifshitz transition associated to the sombrero shaped saddle points of the valence band when the flake thickness is reduced to a few nanometers;[19] our findings are also relevant to the design and fabrication of optical and electronic devices based on InSe, whose performance can be degraded by carrier localization on strongly confined dopant states.

[1]A. K. Geim and I. V. Grigorieva, Nature **499**, 419 (2013).

[2]K. S. Novoselov, Rev. Mod. Phys. **83**, 837 (2011).

[3]K. S. Novoselov, D. Jiang, F. Schedin, T. J. Booth, V. V. Khotkevich, S. V. Morozov, and A. K. Geim, Proc. Natl. Acad. Sci. USA **102**, 10451 (2005).

[4]L. Britnell, R. V. Gorbachev, R. Jalil, B. D. Belle, F. Schedin, A. Mishchenko, T. Georgiou, M. I. Katsnelson, L. Eaves, S. V. Morozov, N. M. R. Peres, J. Leist, A. K. Geim, K. S. Novoselov, and L. A. Ponomarenko, Science **335**, 947 (2012).

[5]T. Georgiou, R. Jalil, B. D. Belle, L. Britnell, R. V. Gorbachev, S. V. Morozov, Y.-J. Kim, A. Gholinia, S. J. Haigh, O. Makarovsky, L. Eaves, L. A. Ponomarenko, A. K. Geim, K. S. Novoselov, and A. Mishchenko, Nat. Nanotechnol. **8**, 100 (2013).

[6]A. Mishchenko, J. S. Tu, Y. Cao, R. V. Gorbachev, J. R. Wallbank, M. T. Greenaway, V. E. Morozov, S. V. Morozov, M. J. Zhu, S. L. Wong, F. Withers, C. R. Woods, Y-J. Kim, K. Watanabe, T. Taniguchi, E. E. Vdovin, O. Makarovsky, T. M. Fromhold, V. I. Fal'ko, A. K. Geim, L. Eaves, and K. S. Novoselov, Nat. Nanotech. **9**, 808–813 (2014).

[7]J. Tse-Wei Wang, J. M. Ball, E. M. Barea, A. Abate, J. A. Alexander-Webber, J. Huang, M. Saliba, I. Mora-Sero, J. Bisquert, H. J. Snaith, and R. J. Nicholas, Nano Lett. **14**, 724 (2014).

[8]J. S. Ross, P. Klement, A. M. Jones, N. J. Ghimire, J. Yan, D. G. Mandrus, T. Taniguchi, K. Watanabe, K. Kitamura, W. Yao, D. H. Cobden, and X. Xu, Nat. Nanotech. **9**, 268 (2014).

[9]J. Xue, J. Sanchez-Yamagishi, D. Bulmash, P. Jacquod, A. Deshpande, K. Watanabe, T. Taniguchi, P. Jarillo-Herrero, and B. J. LeRoy, Nat. Mater. **10**, 282 (2011).

[10]M. Yankowitz, J. Xue, D. Cormode, J. D. Sanchez-Yamagishi, K. Watanabe, T. Taniguchi, P. Jarillo-Herrero, P. Jacquod, and B. J. LeRoy, Nat. Phys. **8**, 382 (2012).

[11]L. A. Ponomarenko, R. V. Gorbachev, G. L. Yu, D. C. Elias, R. Jalil, A. A. Patel, A. Mishchenko, A. S. Mayorov, C. R. Woods, J. R. Wallbank, M. Mucha-Kruczynski, B. A. Piot, M. Potemski, I. V. Grigorieva, K. S. Novoselov, F. Guinea, V. I. Falko, and A. K. Geim, Nature **497**, 594 (2013).

[12]C. R. Dean, L. Wang, P. Maher, C. Forsythe, F. Ghahari, Y. Gao, J. Katoch, M. Ishigami, P. Moon, M. Koshino, T. Taniguchi, K. Watanabe, K. L. Shepard, J. Hone, and P. Kim, Nature **497**, 598 (2013).

[13]B. Hunt, J. D. Sanchez-Yamagishi, A. F. Young, M. Yankowitz, B. J. LeRoy, K. Watanabe, T. Taniguchi, P. Moon, M. Koshino, P. Jarillo-Herrero, and R. C. Ashoori, Science **340**, 1427 (2013).

[14]G. W. Mudd, S. A. Svatek, T. Ren, A. Patanè, O. Makarovsky, L. Eaves, P. H. Beton, Z. D. Kovalyuk, G. V. Lashkarev, Z. R. Kudrynskyi, and A. I. Dmitriev, Adv. Mater. **25**, 5714 (2013).

[15]S. Lei, L. Ge, S. Najmaei, A. George, R. Kappera, J. Lou, M. Chhowalla, H. Yamaguchi, G. Gupta, R. Vajtai, A. D. Mohite, and P. M. Ajayan, ACS Nano **8**, 1263 (2014).

[16]S. R. Tamalampudi, L. Yi-Ying, K. U. Rajesh, S. Raman, L. Chun-Da, M. B. Karukanara, C. Che-Hsuan, C. C. Fang, and C. Yit-Tsong, Nano Lett. **14**, 2800 (2014).

[17]N. Balakrishnan, Z. R. Kudrynskyi, M. W. Fay, G. W. Mudd, S. A. Svatek, O. Makarovsky, Z. D. Kovalyuk, L. Eaves, P. H. Beton, and A. Patanè, Adv. Opt. Mater. **2**, 1064 (2014).

[18]W. Feng, W. Zheng, W. Cao, and P. A. Hu, Adv. Mater. **26**, 6587 (2014).

[19]V. Zólyomi, N. D. Drummond, and V. I. Falko, Phys. Rev. B **89**, 205416 (2014).

[20]J. F. Sánchez-Royo, G. Muñoz-Matutano, M. Brotons-Gisbert, J. P. Martínez-Pastor, A. Segura, A. Cantarero, R. Mata, J. Canet-Ferrer, G. Tobias, E. Canadell, J. Marqués-Hueso, and B. D. Gerardot, Nano Res. **7**, 1556 (2014).

[21]E. Kress-Rogers, R. J. Nicholas, J. C. Portal, and A. Chevy, Solid State Commun. **44**, 379 (1982).

[22]F. Manjón, A. Segura, V. Muñoz-Sanjosé, G. Tobías, P. Ordejón, and E. Canadell, Phys. Rev. B **70**, 125201 (2004).

[23]A. Segura, K. Wünstel, and A. Chevy, Appl. Phys. A **31**, 139 (1983).

[24]E. Kress-Rogers, G. F. Hopper, R. J. Nicholas, W. Hayes, J. C. Portal, and A. Chevy, J. Phys. C **16**, 4285 (1983).

[25]J. Martinez-Pastor, A. Segura, C. Julien, and A. Chevy, Phys. Rev. B **46**, 4607 (1992).

[26]A. A. Homs and B. Marí, J. Appl. Phys. **88**, 4654 (2000).

[27]C. Ferrer-Roca, A. Segura, M. V. Andrés, J. Pellicer, and V. Muñoz, Phys. Rev. B **55**, 6981 (1997).

[28]G. Bastard, Phys. Rev. B **24**, 4714 (1981).

[29]B. Abay, H. S. Güder, H. Efeoğlu, and Y. K. Yoğurtçu, J. Phys. D: Appl. Phys. **32**, 2942 (1999).